

Electronic Supplementary Information

Electrosynthesis of amino acids from biomass- derived α -hydroxyl acids

Kaili Yan, Morgan L. Huddleston, Brett A. Gerdes, and Yujie Sun*

Department of Chemistry, University of Cincinnati, Cincinnati, OH 45221, United States

Table of contents

Fig. S1 (a-c) Cyclic voltammograms of DL-mandelic acid oxidation in the presence of NHPI and different organic bases: (a) Et ₃ N, (b) pyridine, and (c) 2,6-lutidine. (d) Comparison on the cyclic voltammograms of DL-mandelic acid oxidation in the presence of NHPI and organic bases (WE: glassy carbon electrode, RE: Ag/Ag ⁺ , CE: Pt wire, one compartment cell; 5 mM NHPI, 25 mM base, 20 mM DL-mandelic acid).	4
Fig. S2 Cyclic voltammograms of DL-mandelic acid oxidation (black line: without DL-mandelic acid; red line: with 20 mM DL-mandelic acid) in the presence of 5 mM NHPI and 25 mM 2,6-lutidine in different electrolytes.	5
Table S1. Summary of DL-mandelic acid oxidation in different electrolytes ^a	5
Fig. S3 Cyclic voltammograms of 5 mM NHPI in the presence of 2.5, 5, 10, 15, 20, 25, and 30 mM 2,6-lutidine in 0.1 M LiClO ₄ MeCN/H ₂ O (v/v: 2/1) (WE: glassy carbon electrode, RE: Ag/Ag ⁺ , CE: Pt wire, one compartment cell; The electrochemical experiments were conducted with five equivalents of 2,6-lutidine versus one equivalent of NHPI).	6
Fig. S4 (a) Cyclic voltammograms of 5 mM NHPI and 25 mM 2,6-lutidine in 0.1 M LiClO ₄ MeCN/H ₂ O (v/v: 2/1) at various scan rates (WE: glassy carbon electrode, RE: Ag/Ag ⁺ , CE: Pt wire, one compartment cell). (b) Peak current of NHPI versus square root of scan rate (The linear dependence of the peak current of NHPI oxidation on the square root of scan rate confirmed that the electrochemical oxidation of NHPI under our experimental condition is a diffusion-controlled and homogenous process).	7
Fig. S5 Cyclic voltammograms of DL-mandelic acid oxidation with different substrate concentration in 0.1 M LiClO ₄ MeCN/H ₂ O (v/v: 2/1) with 5 mM HNPI and 25 mM 2,6-lutidine (WE: glassy carbon electrode, RE: Ag/Ag ⁺ , CE: Pt wire, one compartment cell).	8
Fig. S6 The mechanism of DL-mandelic acid oxidation mediated by NHPI in the presence of 2,6-lutidine (B).	9
Fig. S7 HPLC calibration curves for (a) DL-mandelic acid detected at 200 nm, (b) phenylglyoxylic acid detected at 245 nm, and (c) benzoic acid detected at 220 nm (Eluent: 5 mM ammonium acetate/acetonitrile (v/v = 95/5); flow rate: 0.5 mL/min).	9
Fig. S8. Proton NMR spectra of phenylglyoxylic acid mixed with NH ₂ OH·HCl before (top) and after (bottom) 24 hours (An oxime intermediate was formed by stirring phenylglyoxylic acid with NH ₂ OH·HCl for 24 hours in 0.1 M LiClO ₄ MeCN/H ₂ O (v/v: 2/1) at room temperature... ..	10
Fig. S9. Proton NMR spectrum of the oxime intermediate, 2-(hydroxyimino)-2-phenylacetic acid after electro-reductive amination at the Ti cathode at -1.0 V vs. Ag/Ag ⁺ with 0.5 equivalent 1,3,5-trimethoxybenzene as the internal standard (Reaction condition: 20 mM 2-(hydroxyimino)-2-phenylacetic acid in 0.1 M LiClO ₄ MeCN/H ₂ O (v/v: 2/1) with Ti, Ag/Ag ⁺ electrode and Pt wire as working, reference and counter electrodes, respectively).	11
Fig. S10 A schematic diagram of our flow electrolysis set up. Error! Bookmark not defined.	
Fig. S11 Proton NMR spectra of the cathode chamber electrolyte obtained from electrolysis of DL-mandelic acid with flow reactor under different applied voltages with 0.5 equivalent 1,3,5-trimethoxybenzene as the internal standard (Anode: carbon paper; cathode: Ti felt; flow rate: 0.8 mL/min).	13

Fig. S12 Proton NMR spectra of commercially purchased DL-3-phenyllactic acid (top), phenylpyruvic acid (middle), and the electrolyte after electrooxidation of DL-3-phenyllactic acid obtained from flow electrolysis at an applied voltage of 2.7 V (bottom) (Anode: carbon paper; cathode: Ti felt; flow rate: 0.8 mL/min; TEMPO as mediator).	14
Fig. S13 (a-b) HPLC trace (a) and calibration curve (b) of the standard phenylpyruvic acid detected at 270 nm. (c) HPLC trace of post-electrolysis solution from the oxidation of 2-hydroxy-3-phenylpropanoic acid (The yield of phenylpyruvic acid was calculated as 92%).	15
Fig. S14 Proton NMR spectra of the cathode chamber electrolyte obtained from electrolysis of DL-3-phenyllactic acid in a flow reactor under applied voltage of 2.7 V with 1 equivalent 1,3,5-trimethoxybenzene as the internal standard (Anode: carbon paper; cathode: Ti felt; flow rate: 0.8 mL/min; TEMPO as mediator).	15
Fig. S15 Proton NMR spectra of commercially purchased glycolic acid (top), glyoxylic acid (middle), and the electrolyte after electrooxidation of glycolic acid obtained from flow electrolysis at an applied voltage of 2.7 V (bottom) with maleic acid as the internal standard (Anode: carbon paper; cathode: Ti felt; flow rate: 0.8 mL/min; NHPI as mediator).	16
Fig. S16 Proton NMR spectra of commercially purchased lactic acid (top), pyruvic acid (middle), and the electrolyte after electrooxidation of lactic acid obtained from flow electrolysis at an applied voltage of 2.7 V (bottom) with maleic acid as the internal standard (Anode: carbon paper; cathode: Ti felt; flow rate: 0.8 mL/min; NHPI as mediator).	17
Fig. S17 Proton NMR spectra of commercially purchased 2-hydroxy-4-methylpentanoic acid (top), 4-methyl-2-oxovaleric acid (middle), and the electrolyte after electrooxidation of 2-hydroxy-4-methylpentanoic acid obtained from flow electrolysis at an applied voltage of 2.7 V (bottom) with maleic acid as the internal standard (Anode: carbon paper; cathode: Ti felt; flow rate: 0.8 mL/min; NHPI as mediator).	188
Fig. S18 Proton NMR spectra of the cathode chamber electrolyte obtained from electrolysis of glycolic acid in a flow reactor under applied voltage of 2.7 V with 0.5 equivalent maleic acid as the internal standard (Anode: carbon paper; cathode: Ti felt; flow rate: 0.8 mL/min).....	19
Fig. S19 Proton NMR spectra of the cathode chamber electrolyte obtained from electrolysis of lactic acid in a flow reactor under applied voltage of 2.7 V with 0.25 equivalent maleic acid as the internal standard (Anode: carbon paper; cathode: Ti felt; flow rate: 0.8 mL/min).....	19
Fig. S20 Proton NMR spectra of the cathode chamber electrolyte obtained from electrolysis of 2-hydroxy-4-methylpentanoic acid in a flow reactor under applied voltage of 2.7 V with 1 equivalent maleic acid as the internal standard (Anode: carbon paper; cathode: Ti felt; flow rate: 0.8 mL/min).	20

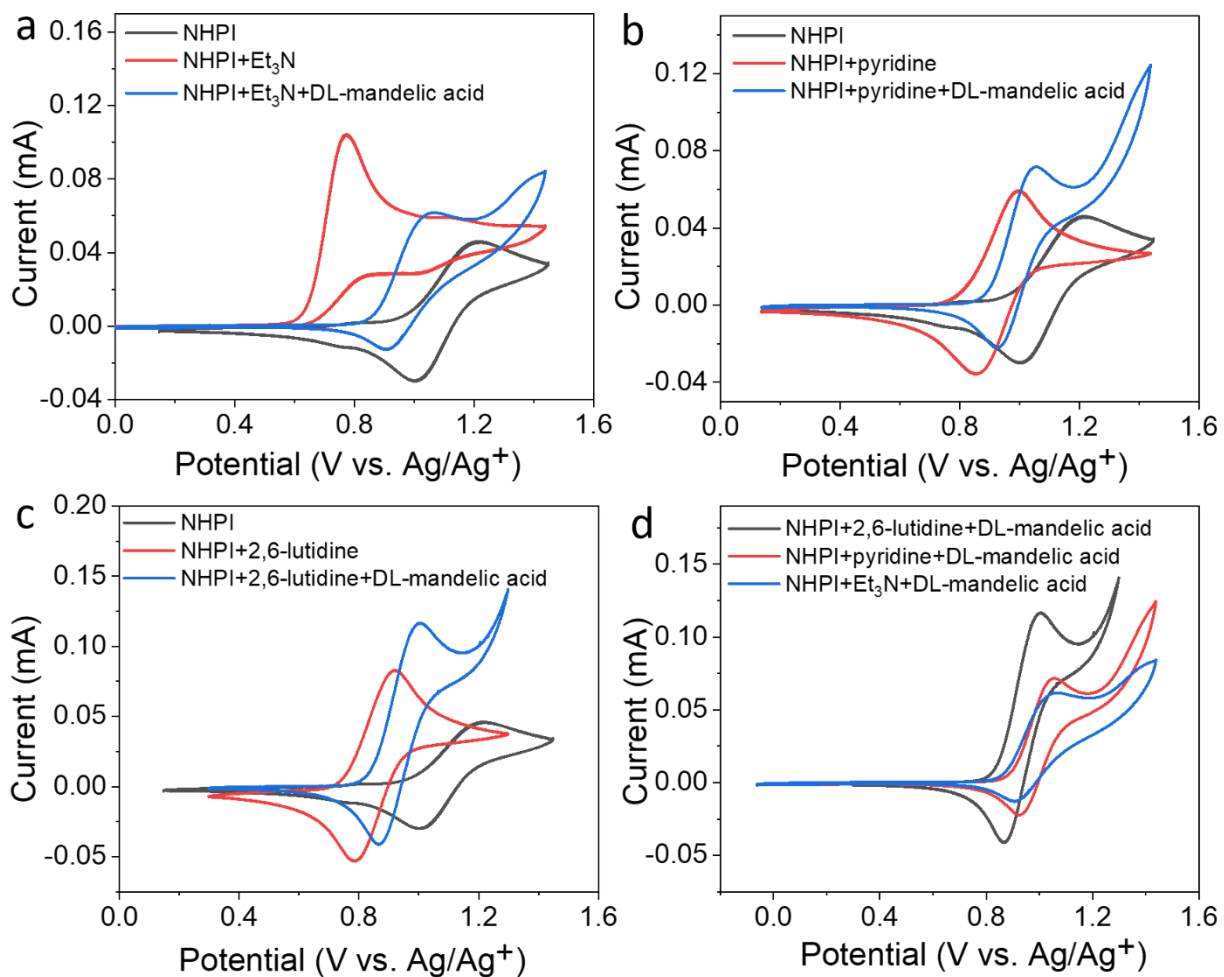


Fig. S1 (a-c) Cyclic voltammograms of DL-mandelic acid oxidation in the presence of NHPI and different organic bases: (a) Et₃N, (b) pyridine, and (c) 2,6-lutidine. (d) Comparison on the cyclic voltammograms of DL-mandelic acid oxidation in the presence of NHPI and organic bases (WE: glassy carbon electrode, RE: Ag/Ag⁺, CE: Pt wire, one compartment cell; 5 mM NHPI, 25 mM base, 20 mM DL-mandelic acid).

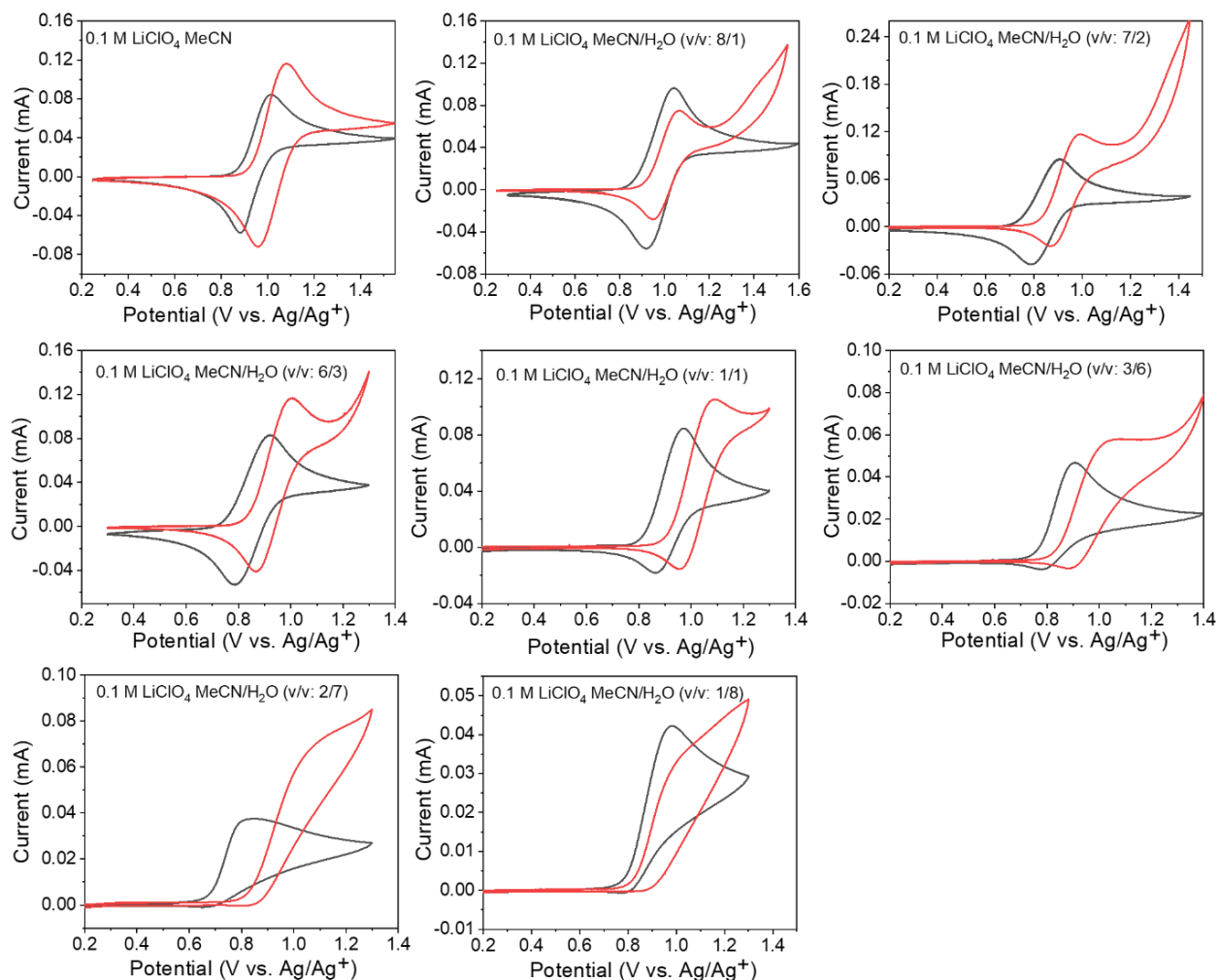


Fig. S2 Cyclic voltammograms of DL-mandelic acid oxidation (black line: without DL-mandelic acid; red line: with 20 mM DL-mandelic acid) in the presence of 5 mM NHPI and 25 mM 2,6-lutidine in different electrolytes.

Table S1. Summary of DL-mandelic acid oxidation in different electrolytes.^a

0.1 M LiClO ₄ MeCN/H ₂ O (v/v)	Yield (%)	Selectivity (%)
9/0	\	\
8/1	\	\
7/2	50	>90
6/3	60	~100
1/1	45	>90
3/6	20	>90
2/7	\	\
1/8	\	\

^a5 mM NHPI, 25 mM 2,6-lutidine, 20 mM DL-mandelic acid, 0.85 V vs. Ag/Ag⁺, theoretical amount of charge passed for the two-electron transfer reaction.

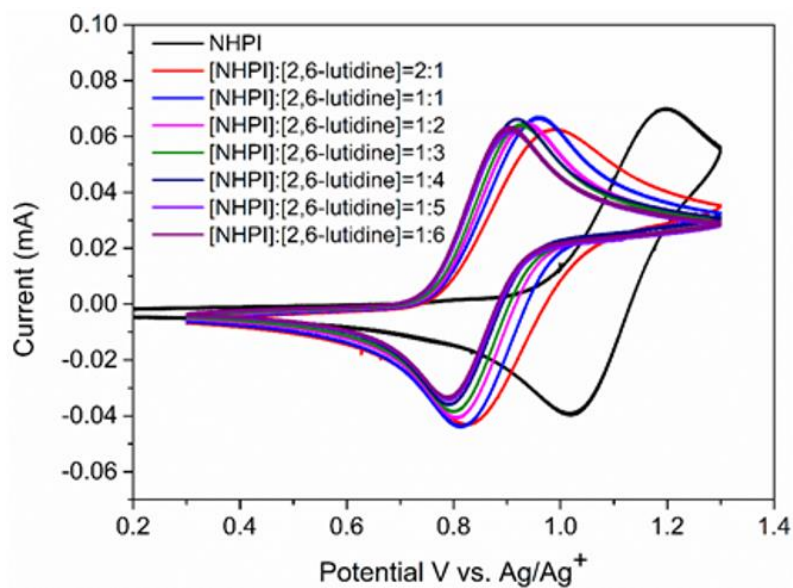


Fig. S3 Cyclic voltammograms of 5 mM NHPI in the presence of 2.5, 5, 10, 15, 20, 25, and 30 mM 2,6-lutidine in 0.1 M LiClO₄ MeCN/H₂O (v/v: 2/1) (WE: glassy carbon electrode, RE: Ag/Ag⁺, CE: Pt wire, one compartment cell; The electrochemical experiments were conducted with five equivalents of 2,6-lutidine versus one equivalent of NHPI).

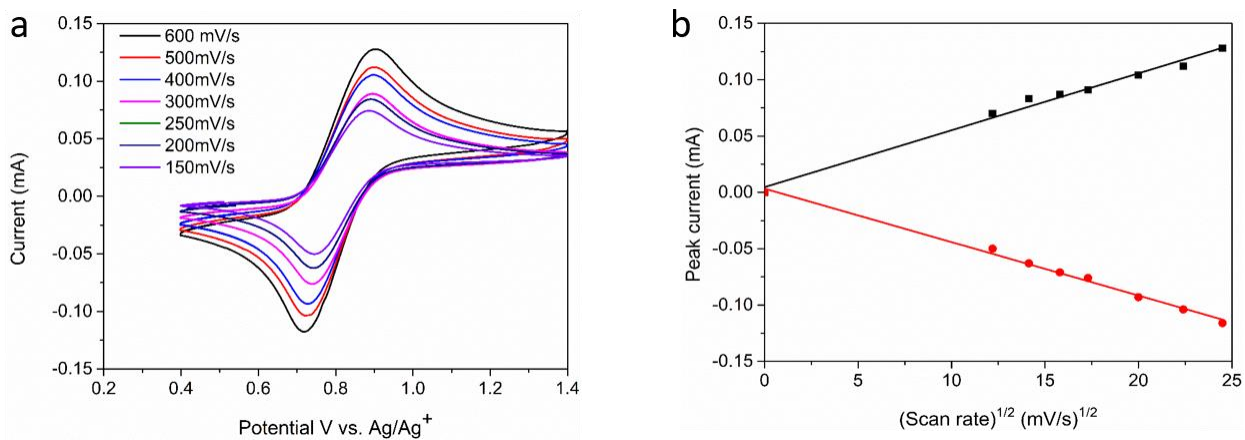


Fig. S4 (a) Cyclic voltammograms of 5 mM NHPI and 25 mM 2,6-lutidine in 0.1 M LiClO₄ MeCN/H₂O (v/v: 2/1) at various scan rates (WE: glassy carbon electrode, RE: Ag/Ag⁺, CE: Pt wire, one compartment cell). (b) Peak current of NHPI versus square root of scan rate (The linear dependence of the peak current of NHPI oxidation on the square root of scan rate confirmed that the electrochemical oxidation of NHPI under our experimental condition is a diffusion-controlled and homogenous process).

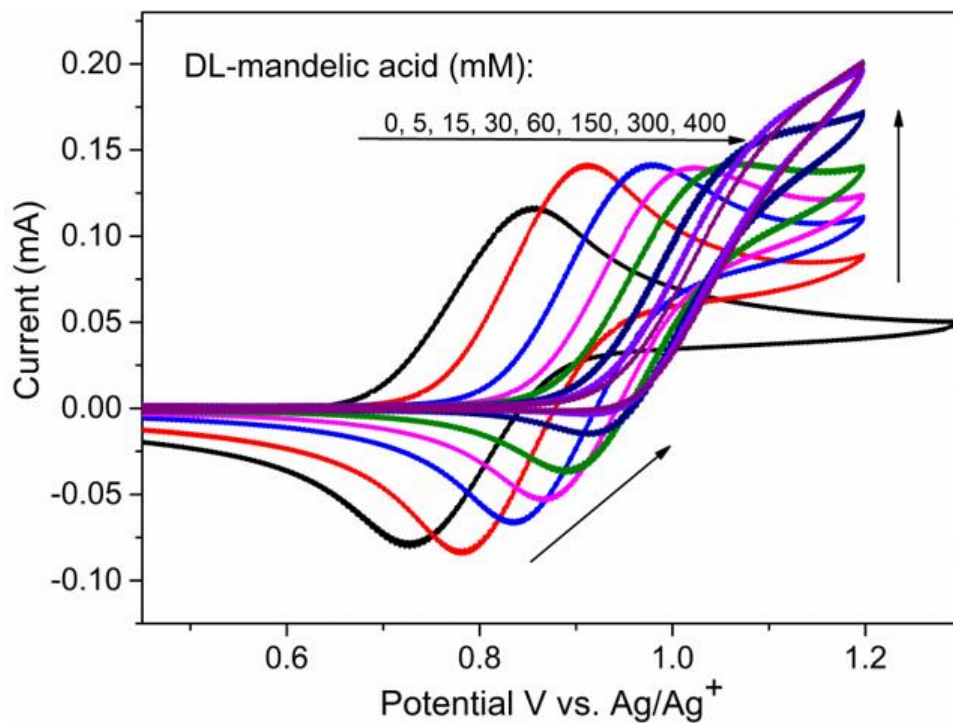


Fig. S5 Cyclic voltammograms of DL-mandelic acid oxidation with different substrate concentration in 0.1 M LiClO₄ MeCN/H₂O (v/v: 2/1) with 5 mM HNPI and 25 mM 2,6-lutidine (WE: glassy carbon electrode, RE: Ag/Ag⁺, CE: Pt wire, one compartment cell).

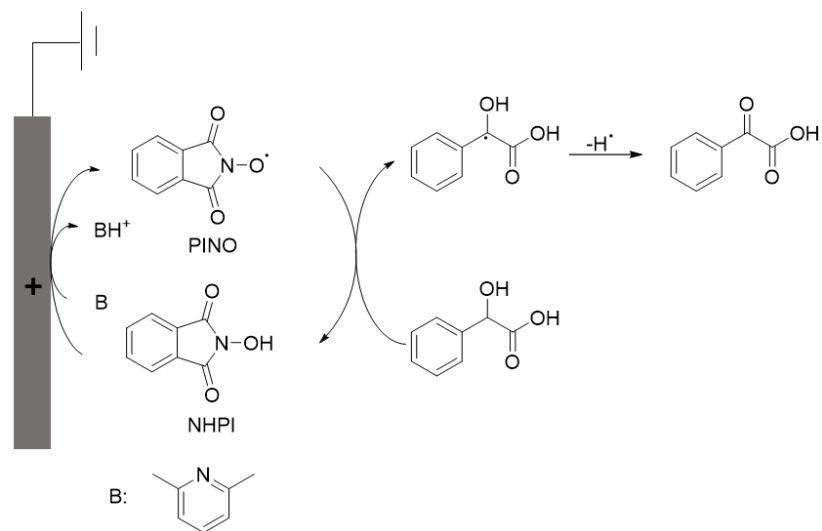


Fig. S6 The mechanism of DL-mandelic acid oxidation mediated by NHPI in the presence of 2,6-lutidine (B).

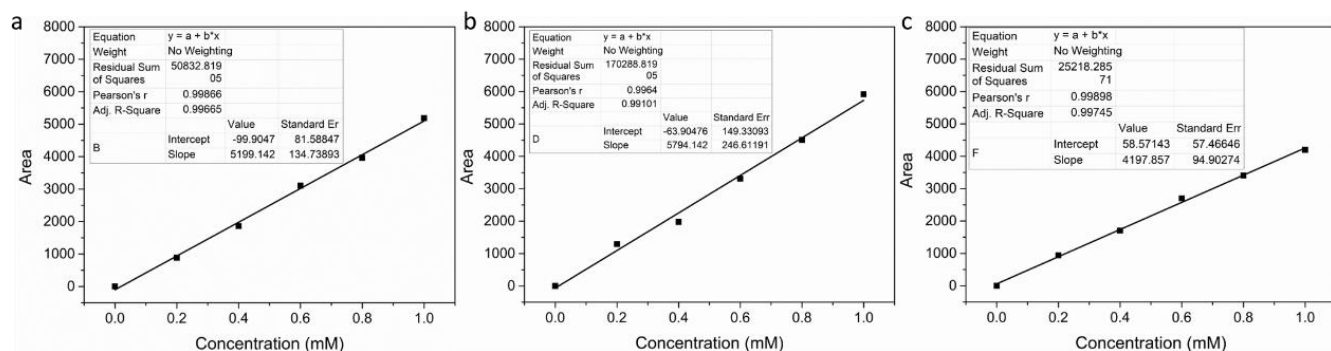


Fig. S7 HPLC calibration curves for (a) DL-mandelic acid detected at 200 nm, (b) phenylglyoxylic acid detected at 245 nm, and (c) benzoic acid detected at 220 nm (Eluent: 5 mM ammonium acetate/acetonitrile (v/v = 95/5); flow rate: 0.5 mL/min).

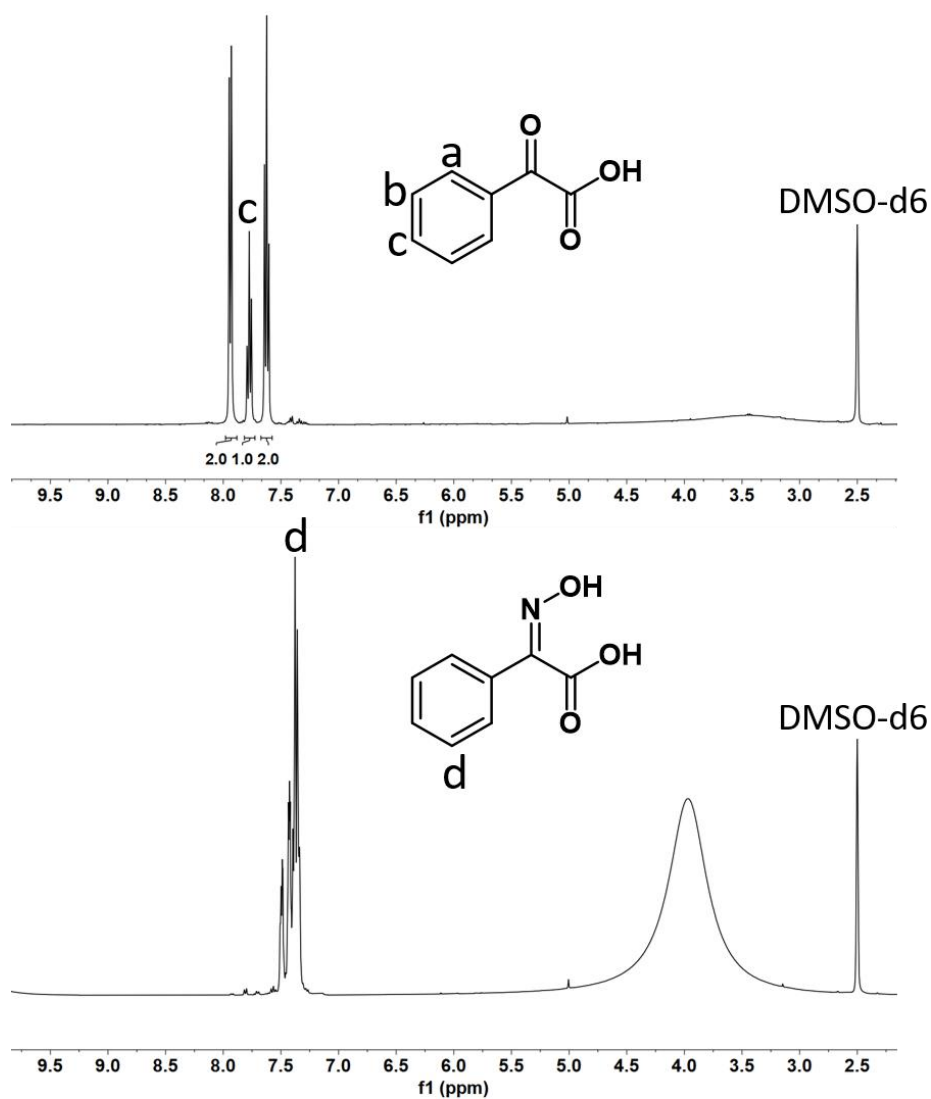


Fig. S8. Proton NMR spectra of phenylglyoxylic acid mixed with $\text{NH}_2\text{OH}\cdot\text{HCl}$ before (top) and after (bottom) 24 hours (An oxime intermediate was formed by stirring phenylglyoxylic acid with $\text{NH}_2\text{OH}\cdot\text{HCl}$ for 24 hours in 0.1 M LiClO_4 MeCN/ H_2O (v/v: 2/1) at room temperature).

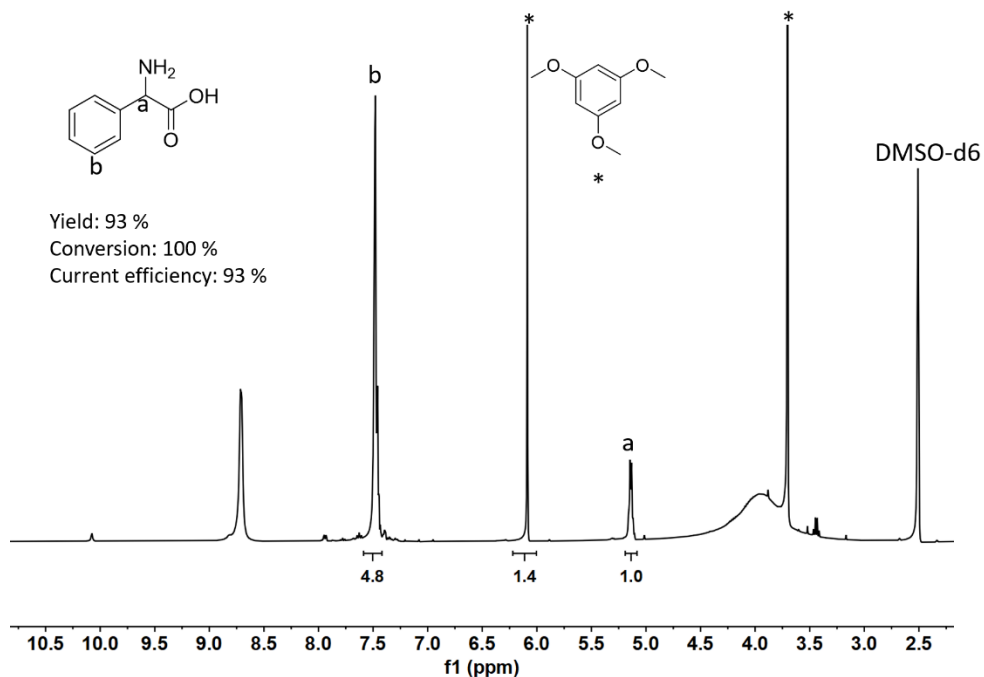


Fig. S9. Proton NMR spectrum of the oxime intermediate, 2-(hydroxyimino)-2-phenylacetic acid after electro-reductive amination at the Ti cathode at -1.0 V vs. Ag/Ag⁺ with 0.5 equivalent 1,3,5-trimethoxybenzene as the internal standard (Reaction condition: 20 mM 2-(hydroxyimino)-2-phenylacetic acid in 0.1 M LiClO₄ MeCN/H₂O (v/v: 2/1) with Ti, Ag/Ag⁺ electrode and Pt wire as working, reference, and counter electrodes, respectively).

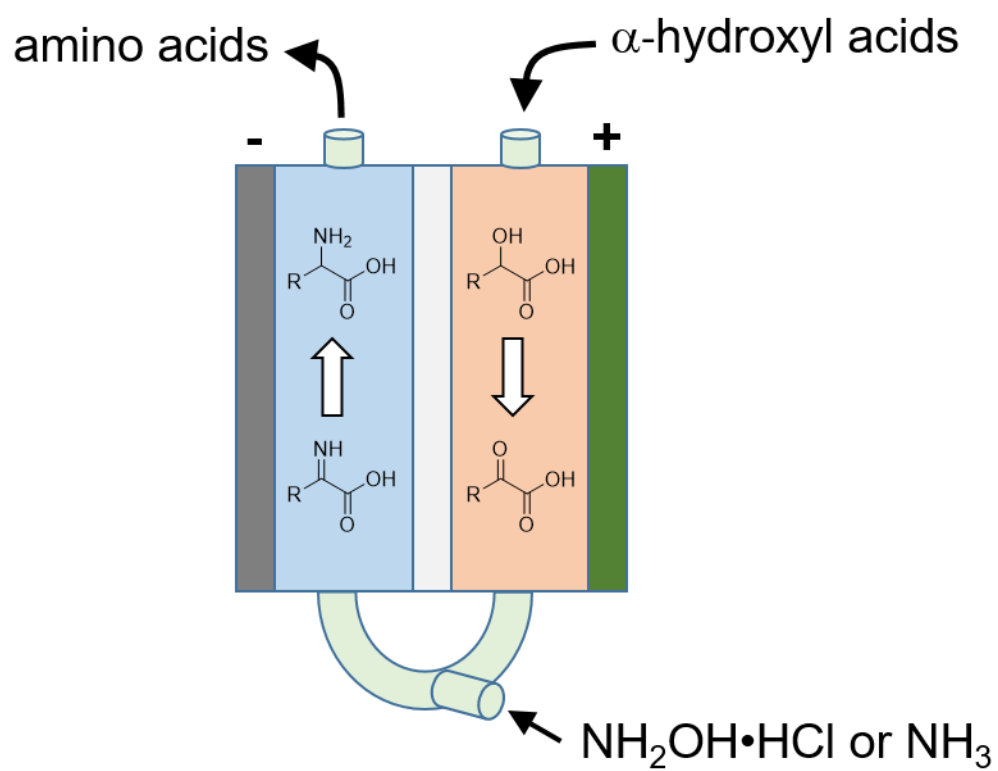


Fig. S10 A schematic diagram of our flow electrolysis set up.

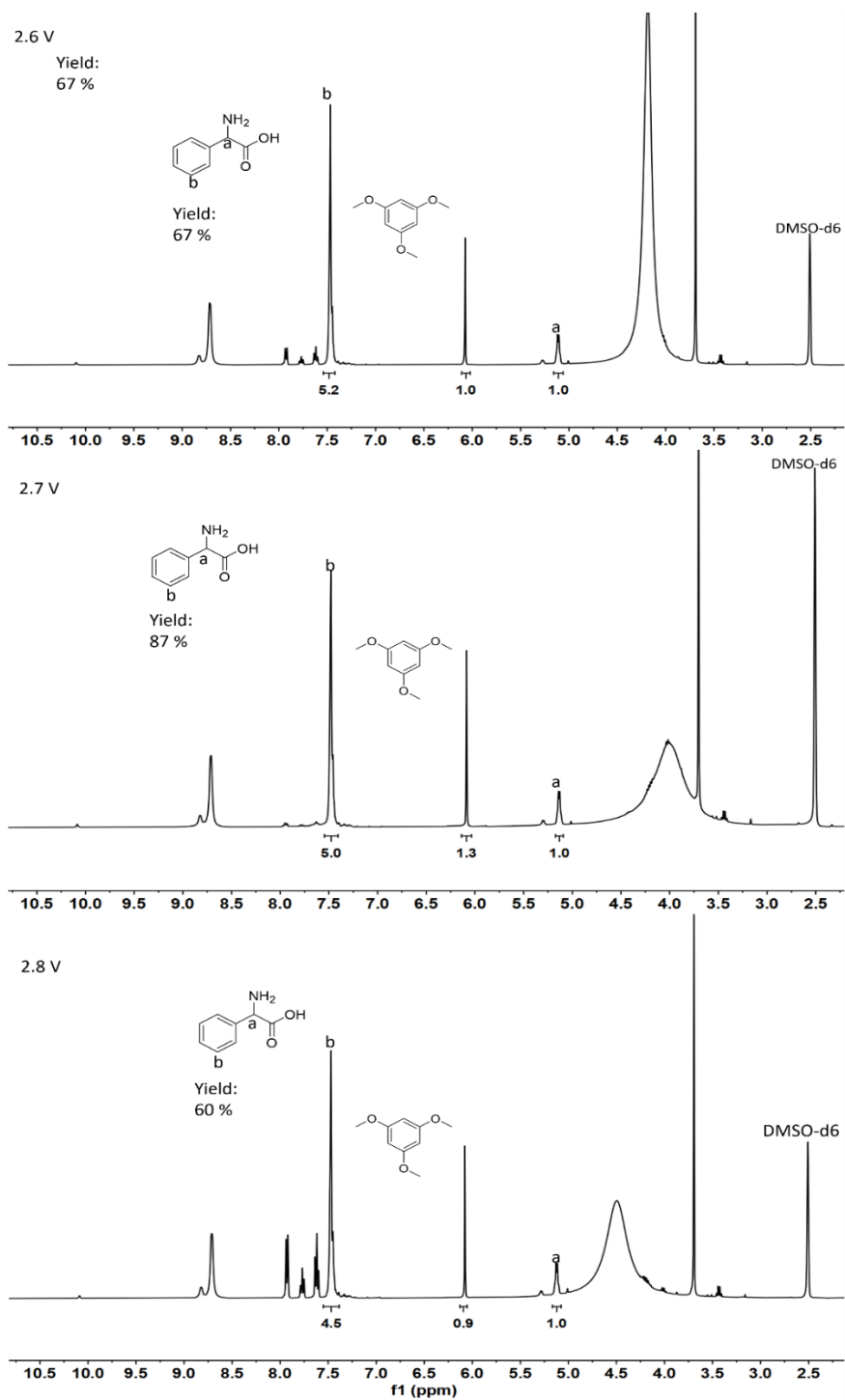


Fig. S11 Proton NMR spectra of the cathode chamber electrolyte obtained from electrolysis of DL-mandelic acid in a flow reactor under different applied voltages with 0.5 equivalent 1,3,5-trimethoxybenzene as the internal standard (Anode: carbon paper; cathode: Ti felt; flow rate: 0.8 mL/min).

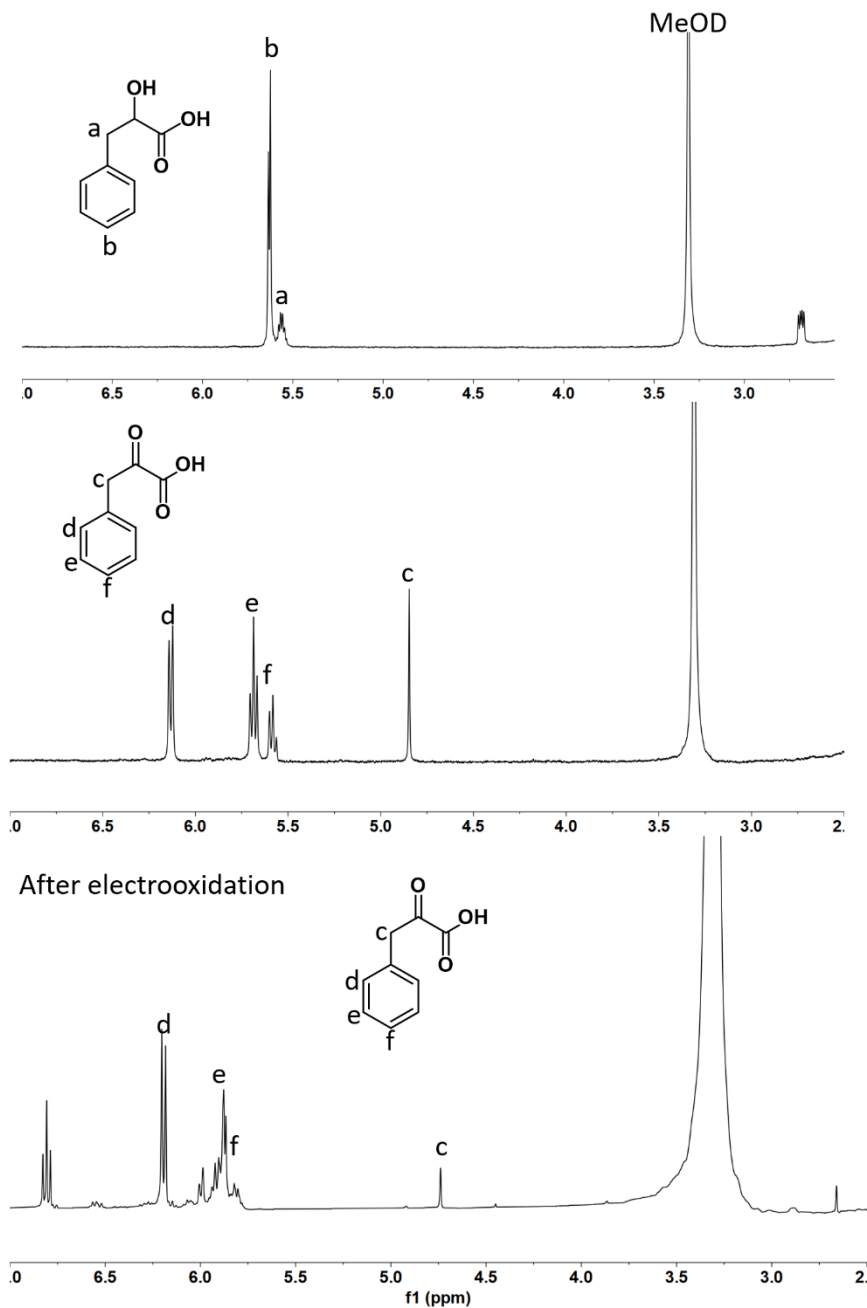


Fig. S12 Proton NMR spectra of commercially purchased DL-3-phenyllactic acid (top), phenylpyruvic acid (middle), and the electrolyte after electrooxidation of DL-3-phenyllactic acid obtained from flow electrolysis at an applied voltage of 2.7 V (bottom) (Anode: carbon paper; cathode: Ti felt; flow rate: 0.8 mL/min; TEMPO as mediator).

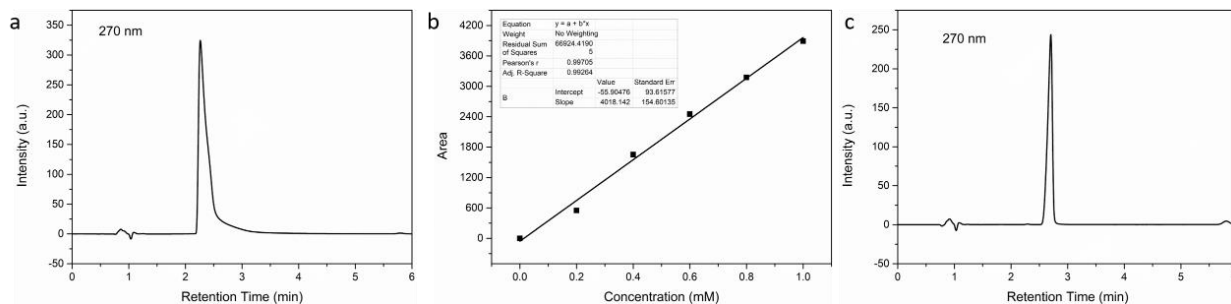


Fig. S13 (a-b) HPLC trace (a) and calibration curve (b) of the standard phenylpyruvic acid detected at 270 nm. (c) HPLC trace of post-electrolysis solution from the oxidation of 2-hydroxy-3-phenylpropanoic acid (The yield of phenylpyruvic acid was calculated as 92%).

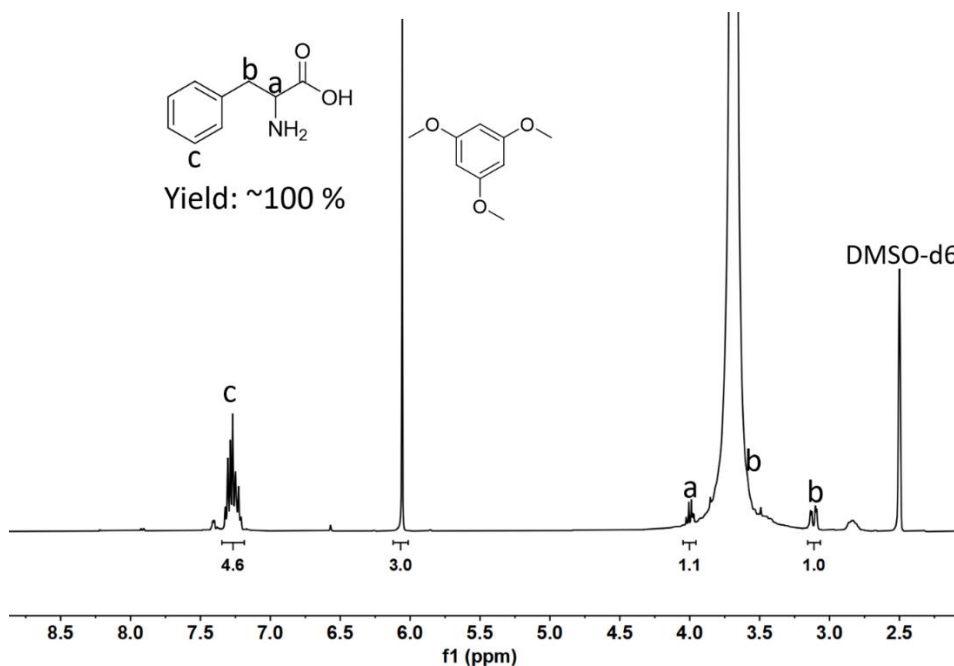


Fig. S14 Proton NMR spectra of the cathode chamber electrolyte obtained from electrolysis of DL-3-phenyllactic acid in a flow reactor under applied voltage of 2.7 V with 1 equivalent 1,3,5-trimethoxybenzene as the internal standard (Anode: carbon paper; cathode: Ti felt; flow rate: 0.8 mL/min; TEMPO as mediator).

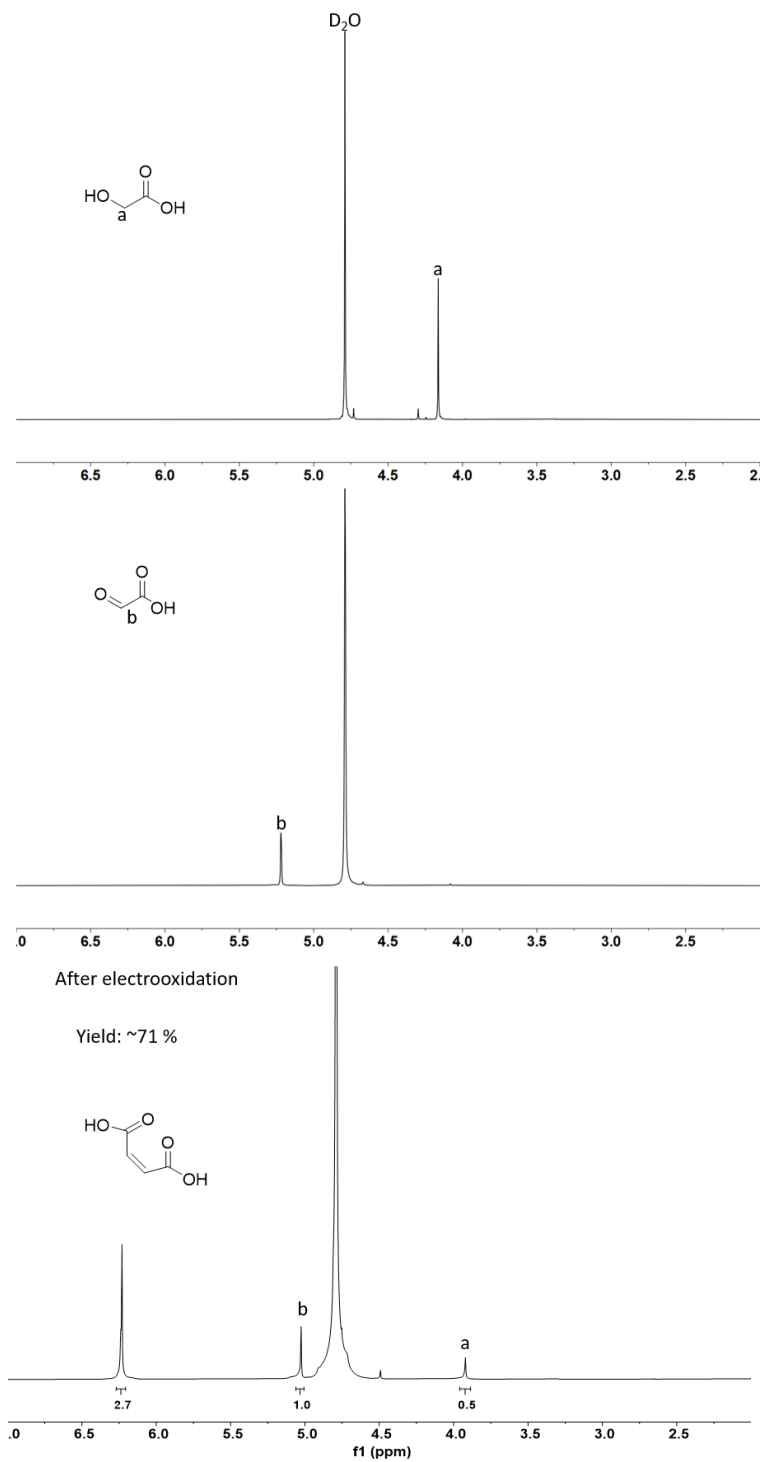


Fig. S15 Proton NMR spectra of commercially purchased glycolic acid (top), glyoxylic acid (middle), and the electrolyte after electrooxidation of glycolic acid obtained from flow electrolysis at an applied voltage of 2.7 V (bottom) with maleic acid as the internal standard (Anode: carbon paper; cathode: Ti felt; flow rate: 0.8 mL/min; NHPI as mediator).

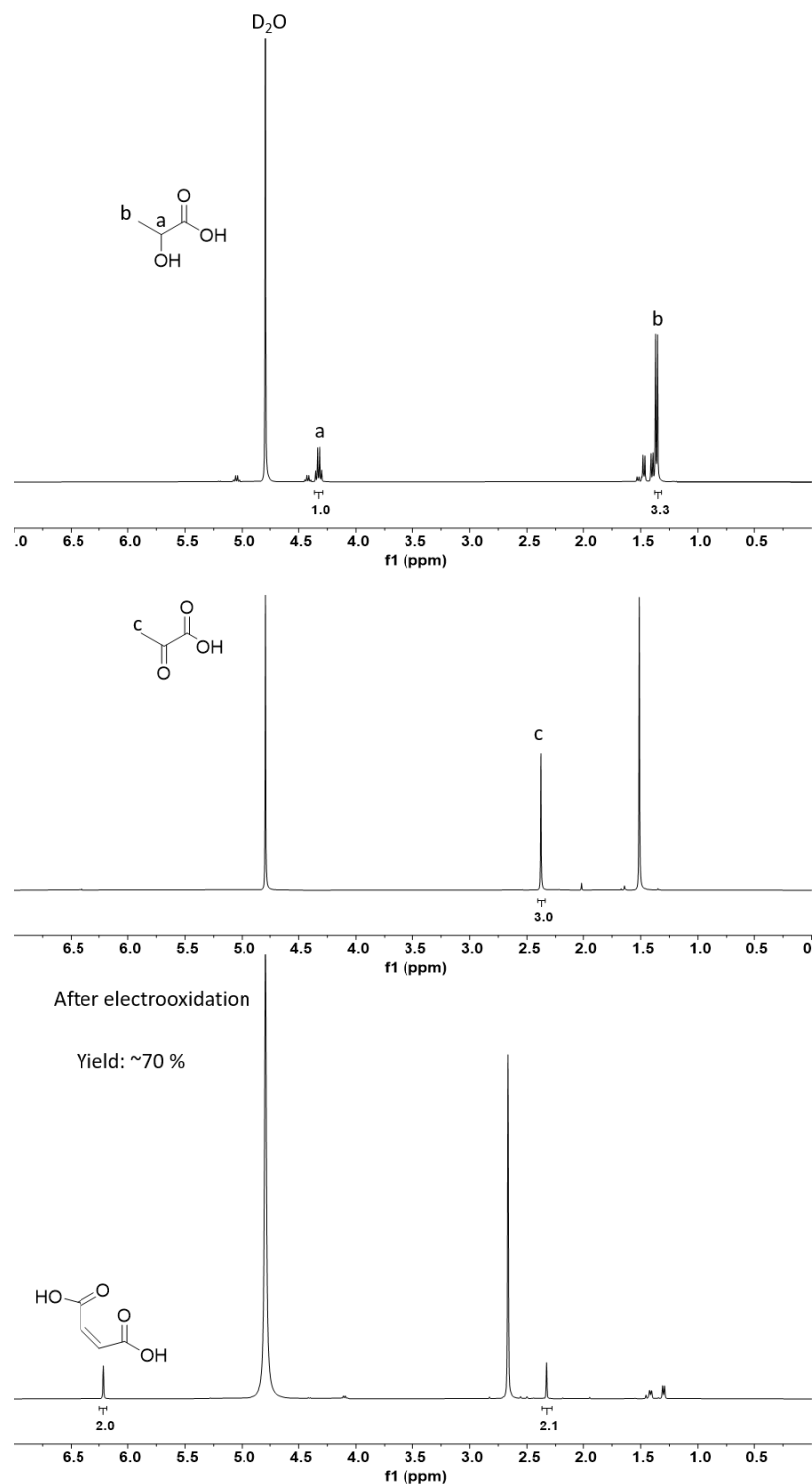


Fig. S16 Proton NMR spectra of commercially purchased lactic acid (top), pyruvic acid (middle), and the electrolyte after electrooxidation of lactic acid obtained from flow electrolysis at an applied voltage of 2.7 V (bottom) with maleic acid as the internal standard (Anode: carbon paper; cathode: Ti felt; flow rate: 0.8 mL/min; NHPI as mediator).

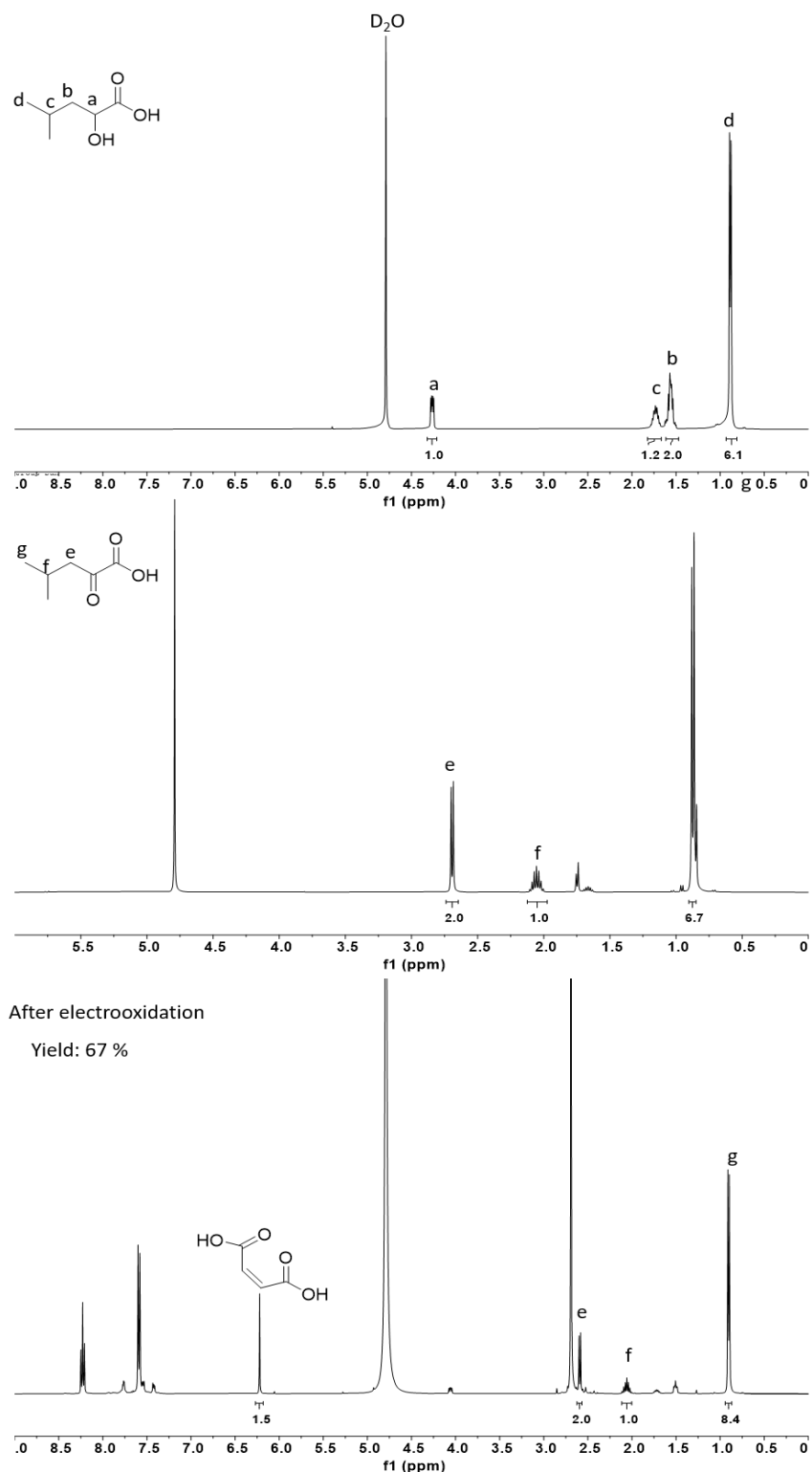


Fig. S17 Proton NMR spectra of commercially purchased 2-hydroxy-4-methylpentanoic acid (top), 4-methyl-2-oxovaleric acid (middle), and the electrolyte after electrooxidation of 2-hydroxy-4-methylpentanoic acid obtained from flow electrolysis at an applied voltage of 2.7 V (bottom) with maleic acid as the internal standard (Anode: carbon paper; cathode: Ti felt; flow rate: 0.8 mL/min; NHPI as mediator).

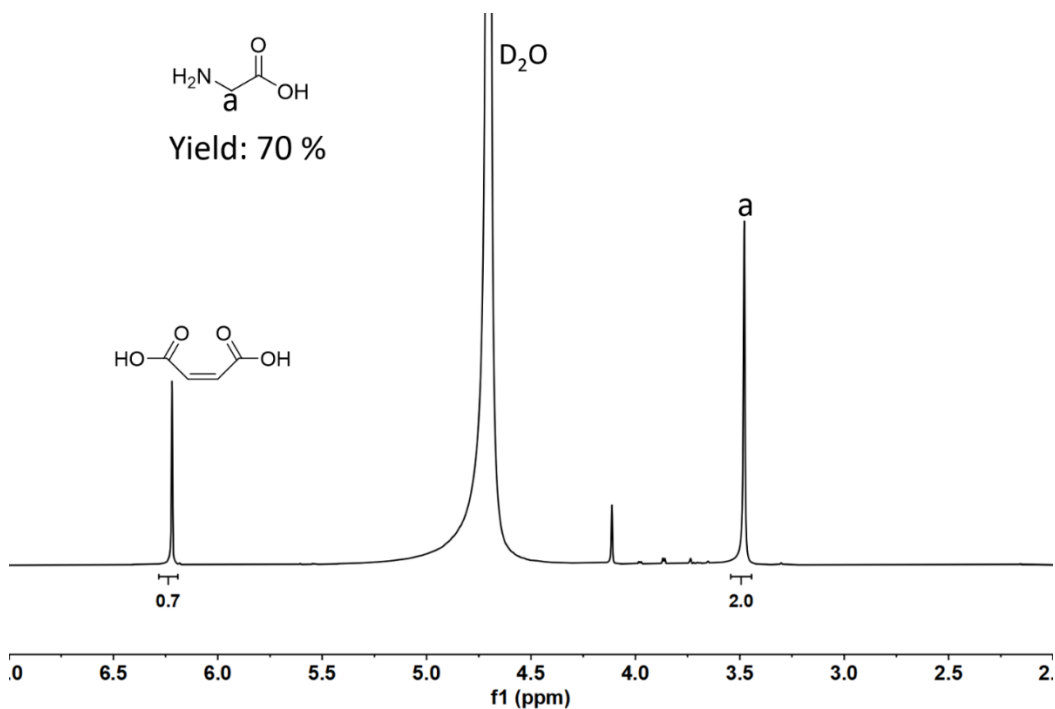


Fig. S18 Proton NMR spectra of the cathode chamber electrolyte obtained from electrolysis of glycolic acid in a flow reactor under applied voltage of 2.7 V with 0.5 equivalent maleic acid as the internal standard (Anode: carbon paper; cathode: Ti felt; flow rate: 0.8 mL/min).

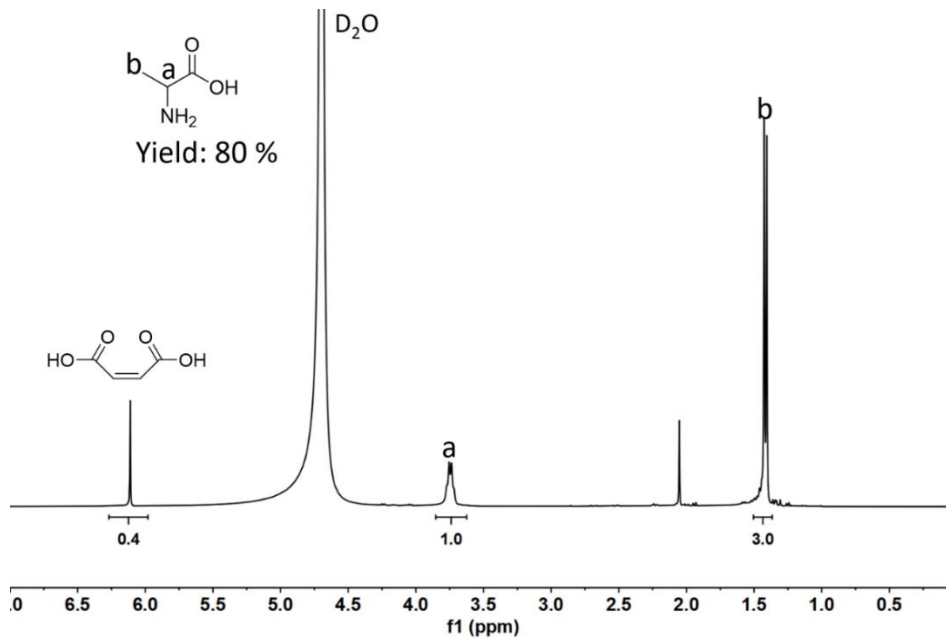


Fig. S19 Proton NMR spectra of the cathode chamber electrolyte obtained from electrolysis of lactic acid in a flow reactor under applied voltage of 2.7 V with 0.25 equivalent maleic acid as the internal standard (Anode: carbon paper; cathode: Ti felt; flow rate: 0.8 mL/min).

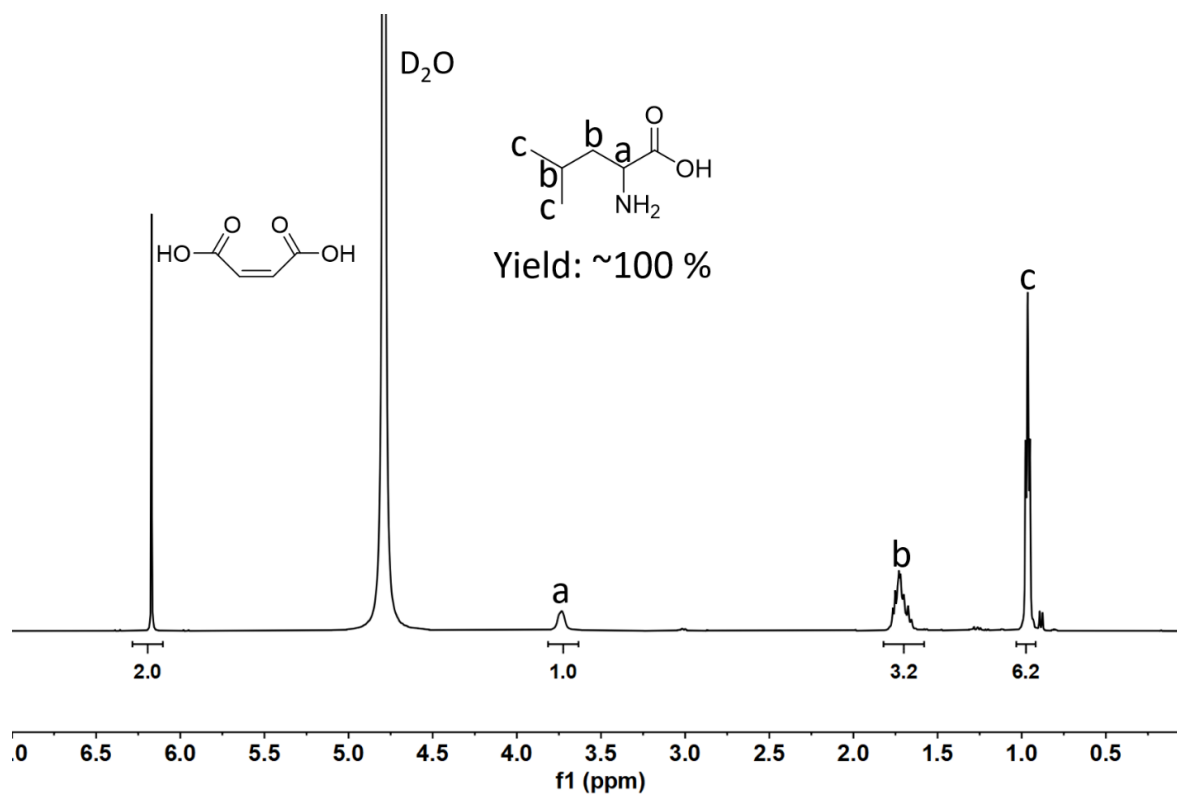


Fig. S20 Proton NMR spectra of the cathode chamber electrolyte obtained from electrolysis of 2-hydroxy-4-methylpentanoic acid in a flow reactor under applied voltage of 2.7 V with 1 equivalent maleic acid as the internal standard (Anode: carbon paper; cathode: Ti felt; flow rate: 0.8 mL/min).